



Validation of FE Modeling for Shallow Reinforced Concrete Beams

Tamer Elrakeeb, Elsayed I. Ismail, A. I. Arfa & K. Z. Soliman

Housing and Building National Research Center, Cairo, Egypt

ملخص البحث

هذا البحث يهدف الي دراسة السلوك اللاخطي في القص للكمرات العريضة المسلحة و الغير مسلحة بكانات رأسيه نظريا. يتكون البرنامج البحث من عدد ثمانية عشر نموذج ثلاثي الابعاد بطريقة العناصر المحددة لكمرات عريضة ذات مقاومة خرسانة مختلفة القيم مع قيم متغيرة لنسبه بحر القص الى العمق. ايضا تم تسليح بعض نماذج الكمرات النظرية بكانات صلب رأسيه مختلفه المساحه والنوع مع ترك البعض بدون كانات. تم مقارنة النتائج النظرية لثلاثة نماذج مع النتائج المعملية لعدد ثلاث كمرات مماثله تم اختبارها سابقا ولوحظ وجود اتفاق جيد بين هذه النتائج من حيث مفاومة القص القصوي و نوعية الانهيار ومنحنيات الحمل مع الترخيم. و بالتالي يمكن استخدام هذه النماذج النظرية لدراسة عدد اكبر من المتغيرات لاحقا. نتائج الدراسة قد تسهم في أخذ التسليح الجذعي في الاعتبار عند تصميم الكمرات العريضة طبقاً للكود المصري للخرسانة مستقبلا.

ABSTRACT

This paper aims at modeling the non-linear shear response of RC wide beams with and without web reinforcement. A total of 18 three dimensional (3D) finite element (FE) models were developed using a computer package ATENA® to perform a parametric study. The accuracy and validity of the computational models have been examined by comparing their predictions with experimental results of three beams published in the literature. The key parameters covered in this investigation are the effect of the existence, amount and yield stress of the vertical stirrups on the shear behavior of RC wide beams. The parameters also included the concrete compressive strength and the shear span to depth ratio. The numerical and experimental results were found to be in good agreement. The numerical models accurately predicted the crack pattern and mid-span deflection of the experimental beams. The FE models can serve as a numerical platform for performance prediction of RC wide beams. The results may contribute to the future development of design guidelines for contribution of the shear reinforcement for wide beams in the Egyptian Concrete Code (ECP 203).

KEYWORDS: Shear strength, Wide beams, Finite element and Modeling.

1 INTRODUCTION

Wide reinforced concrete beams and thick slabs are frequently used as economical transfer elements when the total structural depth is limited. The wide beams may be used to carry direct forces, or to serve as primary transfer elements. A system of wide beams may provide a simple and economical solution to transfer column loads from the tower portion over required column free spaces in the podium or parking areas below. Thick one-way transfer slabs can serve similar roles when the column layout to be transferred is irregular in the plan and for roofs of under-ground stations [1-4]. In Egypt, it is a common practice to utilize floor systems consisting of hollow block slabs resting on embedded wide beams having the same depth as that of the hollow block slabs.

Recently, some researchers directed their efforts to study the shear behavior of wide beams. Lubell et al [1] investigated the influence of the shear reinforcement spacing on the one-way shear capacity of wide reinforced concrete members. A series of 13 normal strength concrete specimens were tested. The specimens contained web reinforcement

ratios close to ACI 318-02 [5] minimum requirements. The study concluded that the effectiveness of the shear reinforcement decreases as the spacing of web reinforcement legs across the width of a member increases. Dino Angelakos et al [3] investigated the effect of concrete strength and minimum stirrups on shear strength of large members. They concluded that changing the concrete strength by a factor of 4 had almost no influence on the shear strength of these large beams while changing the longitudinal reinforcement ratio from 0.5 to 2.09% increased the observed shear strength by 62%. Khalil [6] carried out an experimental study to investigate the shear behavior of wide beams in hollow block slabs. It was concluded that the shear capacity of wide beam with shear reinforcement reached as high as 300% of those without shear reinforcement. The study did not mention any test results about the ductility of the tested beams. On the other hand, the behavior of reinforced concrete wide beams with diverse types of reinforcement was investigated by Seyed Esmail et al [7]. The results revealed that using some numbers of independent bent-up bars significantly improved the shear capacity of wide beams. The combination of independent bent-up bars with stirrups led to higher shear capacity and gradual failure of the specimen. Independent horizontal bars increased the shear capacity to some extent, but the beam was less ductile through failure. The results also indicated that the beam with banded main reinforcement achieved a larger failure load than did the beam with evenly distributed main bars.

In spite of the research efforts directed to the shear capacity of concrete, there is still great discord concerning the mechanisms that govern shear in concrete. Proposed theories vary radically from the simple 45° truss model to the very complex non-linear fracture mechanics. Yet nearly all the resulting design procedures are empirical or semi-empirical at best and are obtained by a regression fit through experimental results or through proposed models using artificial neural network. Moreover, there is great discrepancy between design codes of different countries. Some of these codes do not even account for some basic and proven factors affecting the shear capacity of concrete members. According to the ECP-203[8], the contribution of shear reinforcement in wide beam is totally discarded and the shear strength provided by concrete equals 67% of the concrete shear strength for slender beams.

This paper presents the development of a detailed 3D nonlinear FE numerical model that can accurately predict the load-carrying capacity and response of RC wide beams, with and without web reinforcement, subjected to four-point bending loading. Also, a parametric study was conducted to evaluate the effect of the existence, yield stress and amount of the vertical stirrups on the shear resistance of RC wide beams. In addition, it presents the effect of the concrete compressive strength and the shear span to depth ratio (a/d). The results may contribute to the future development of design guidelines for contribution of the shear reinforcement for wide beams in the ECP 203[8].

2 DETAILS OF SPECIMENS

The experimental results of three RC wide beams published by Said et al [9] have been used in the present study for verification of the numerical results. The three beams were of 30 MPa concrete cube compressive strength. They were 700 mm wide, 250 mm deep, 1750 mm long and tested at a shear span of 600 mm with a shear span-depth ratio (a/d) equal to 3.0. High strength steel, grade 40/60, of 10, 12 and 22 mm diameter (denoted by T) was used in the experimental tests. Mild steel, grade 24/35, of 6 mm diameter (denoted by R) was also used. All the specimens were reinforced with identical longitudinal steel bars. In order to investigate the shear behavior, the

specimens were designed to fail in shear (i.e., the flexural capacity was designed to exceed the shear capacity of the tested beams). Beam SB1 represents the control specimen with no web reinforcement. The amount of transverse reinforcement in the other specimens was varied by varying the diameter of the stirrups. Typical concrete dimensions and reinforcement details of the test specimens are illustrated in Fig. 1-a and Table 1.

The three specimens were instrumented to measure the applied load, mid-span deflection, and strains of vertical reinforcement in the constant shear force region. A linear variable displacement transducer (LVDT) for measuring deflection was mounted at the bottom side of the midspan for each specimen. Load was applied using a hydraulic jack and it was distributed equally by a spreader beam to two points along the specimen. The test was continued after the ultimate load in order to evaluate the post peak behavior of the tested beams. The development of cracks was marked along the sides of the specimens. The numerical analysis of these three beams was verified with experimental results and then extended to carry out a parametric study. The effective depth and width of beams and also the longitudinal reinforcement were kept constant. Table 1 summarizes the configuration of the FE models and variables of the parametric study. The specimens are designated as *a-b-c* where *a* is the number of the beam, *b* is the value of (*a/d*) and *c* is the concrete grade.

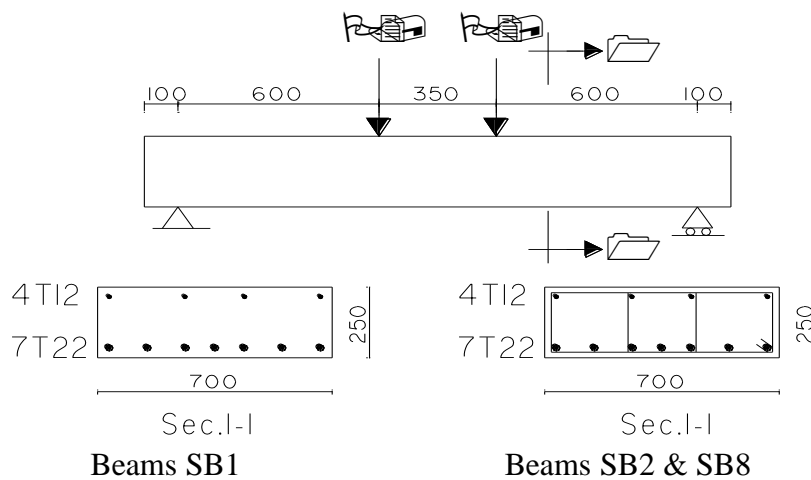


Fig. 1-a: Details of the tested beams

2.1 Finite Element Modeling

A total of eighteen 3D FE models were developed. The concrete was modelled using 3D solid brick elements. The steel bars were modeled as “discrete reinforcement” using truss elements. A sensitive study has been performed to analyze the effect of mesh size and it was found that reducing the element size less than 15mm had an insignificant effect on numerical results. The finite element model is shown in Fig 1.b. The steel loading plates adopted in the FE model covered the entire width of the beam. The model is supported on two plates, one at each side. One end support plate was restrained from movement in the vertical direction (Z) and in the out plan direction (Y) with a line support placed at the bottom center of the plate. The other support is restrained in all directions (Z, X and Y) to maintain the model stability and prevent the out of plan distortion.

The beams were divided into six groups G1 to G6 based on their concrete strength and (a/d) ratio. Each group has three beams, one without web reinforcement to act as a control and the remaining two specimens were reinforced with R6/200 mm and T10/200 mm, respectively. A displacement-controlled incremental loading method was employed in the analysis. An iterative solution procedure based on the Newton-Raphson method was adopted in the analysis.

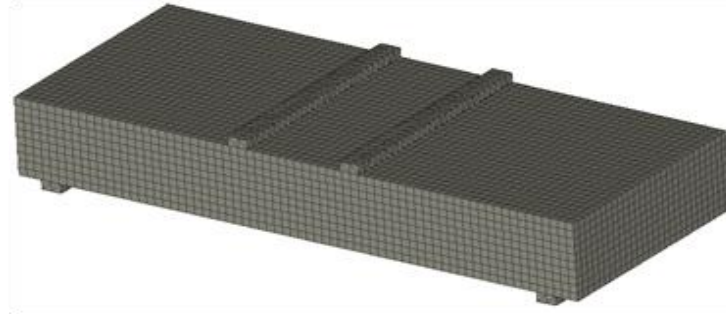


Fig.1-b Three dimensional FE model

Table 1: Configuration of the FE models and results

Group	Beam	Stirrups, A_{st}	f_{cu} , MPa	a/d	Ultimate load, P_u (kN)			Δ_u mm		Ductility (kN.mm)
					Theo.	Exp	Gain* %	Theo.	Exp	Theo.
G1	SB1-3-30	----	30	3	508.7	450	---	2.75	5.5	863
	SB2-3-30	R6/200 mm			582.5	596	14.5	3.17	4.8	1085
	SB8-3-30	T10/200 mm			700.0	807	37.7	5.72	9.1	2860
G2	SB1-2-30	----	30	2	634.4	---	---	3.67	---	1893
	SB2-2-30	R6/200 mm			753.1	---	18.77	4.32	---	2480
	SB8-2-30	T10/200 mm			987.9	---	55.59	5.67	---	4330
G3	SB1-3-45	----	45	3	628.8	---	---	3.33	---	1225
	SB2-3-45	R6/200 mm			667.9	---	7.21	3.54	---	1465
	SB8-3-45	T10/200 mm			826.0	---	31.36	5.68	---	3660
G4	SB1-2-45	----	45	2	797.3	---	---	4.38	---	2960
	SB2-2-45	R6/200 mm			906.5	---	13.73	4.82	---	3070
	SB8-2-45	T10/200 mm			1168.6	---	46.55	6.18	---	5120
G5	SB1-3-60	----	60	3	654.3	---	---	3.28	---	1290
	SB2-3-60	R6/200 mm			711.7	---	8.71	3.73	---	1580
	SB8-3-60	T10/200 mm			857.3	---	31.04	6.13	---	4040
G6	SB1-2-60	----	60	2	900.0	---	---	4.12	---	3640
	SB2-2-60	R6/200 mm			941.9	---	4.66	4.51	---	4330
	SB8-2-60	T10/200 mm			1252.6	---	39.1	6.78	---	6980

* Relative to SB1 of the same group, theoretically.

2.2 Material Constitutive Laws

The 3D non-linear cementations material model of the FE package ATENA [10] was used in the analysis. The model combines constitutive laws for tensile (fracturing) and compressive (plastic) behavior. The uniaxial stress-strain and tensile softening laws are shown in Fig. 2. The peak values of the stress in compression, f_{cp} , and tension, f_{tp} , are derived from a triaxial failure function. The ascending branch of the stress-strain relationship of concrete in compression is based on the CEB-FIP Model Code [11]. The softening concrete law in compression is assumed linearly descending based on the work conducted by Van Mier [12]. The hardening/softening plasticity model is based on Men etrey-Willam failure surface. The fracture model is based on the classical orthotropic smeared crack formulation and crack band model. It employs Rankine failure criterion and exponential softening based on crack opening. The fixed crack model has been adopted in the present study. The crack opening displacement, w_t , is derived from the fracture strain, ϵ_f , and the crack band length, L_t . The crack opening at the complete release of stress, w_{tc} , is based on the fracture energy of the concrete needed to create a unit area of stress-free crack, G_f , and the peak value of stress in tension, f_{tp} .

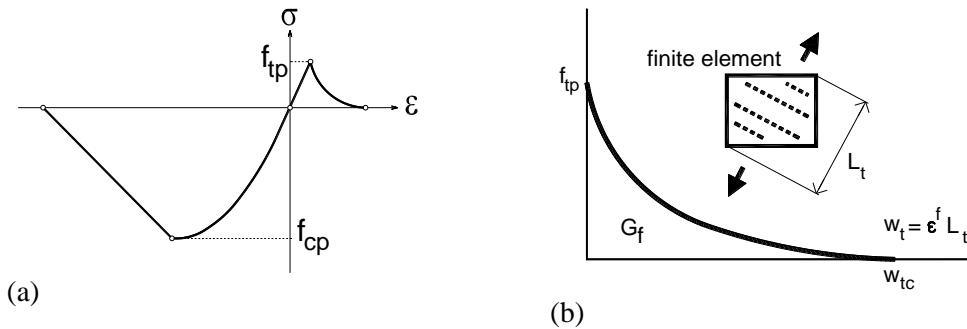


Fig. 2: Concrete model: (a) uniaxial stress-strain relationship, (b) tensile softening law

The tensile strength and young's modulus of the concrete are taken as per the EN 1992-1-1 (European Committee for Standardization), [13]. The Poisson's ratio of the concrete is assumed as 0.2. Shear and compressive strengths of a cracked concrete are calculated using the Modified Compression Field Theory of Vecchio and Collins [14]. The strength reduction function is given in  ervenka et al. [10]. The stress-strain response of the steel reinforcement is assumed bilinear stress-strain relationship that considers strain hardening which allows the stresses to increase after yielding. The input parameters for the bilinear constitutive model are the modulus of elasticity E_s , the yield strength f_y , and the hardening parameters which were considered as the default values in ATENA [10]. ATENA gives the load deflection curve, the ultimate load, the ultimate deflection and the cracking behavior.

3 TEST RESULTS

3.1 Cracking Behavior and Mode of Failure

The Specimens SB1-3-30 and SB2-3-30 failed in a mode of shear failure characterized by diagonal shear tension mode of failure. The behavior of the SB8-3-30 was characterized by diagonal shear mode of failure accompanied with crushing of the web concrete and this failure may be called shear compression failure. The crack pattern of the sample specimens at failure were predicted numerically and compared to

those obtained from the experiments in Fig.3. There is a good correlation between the predicted and experimental crack patterns.

3.2 Load capacity

Table 1 summarizes the results of the tested beam specimens. The table gives the load capacity P_u and the corresponding deflection Δ_u of the tested beams which were measured experimentally and predicted numerically to verify the analytical model. All the predicted strengths were in the range of 13% error band which confirms the ability of the numerical models to accurately predict the load capacity of the wide beams with and without web reinforcement. Expectedly, the control beams SB1, with no web reinforcement, had the lowest ultimate load values compared with the other beams with web reinforcement providing the same value of f_{cu} and (a/d) . Beam SB8-2-60 with vertical stirrups of T10/200 mm, $f_{cu} = 60\text{MPa}$ and $(a/d) = 2$ showed the highest ultimate load of 1252.6 kN. Among the tested specimens, beam SB8-2-60 recorded the highest value of ultimate displacement = 6.8 mm.

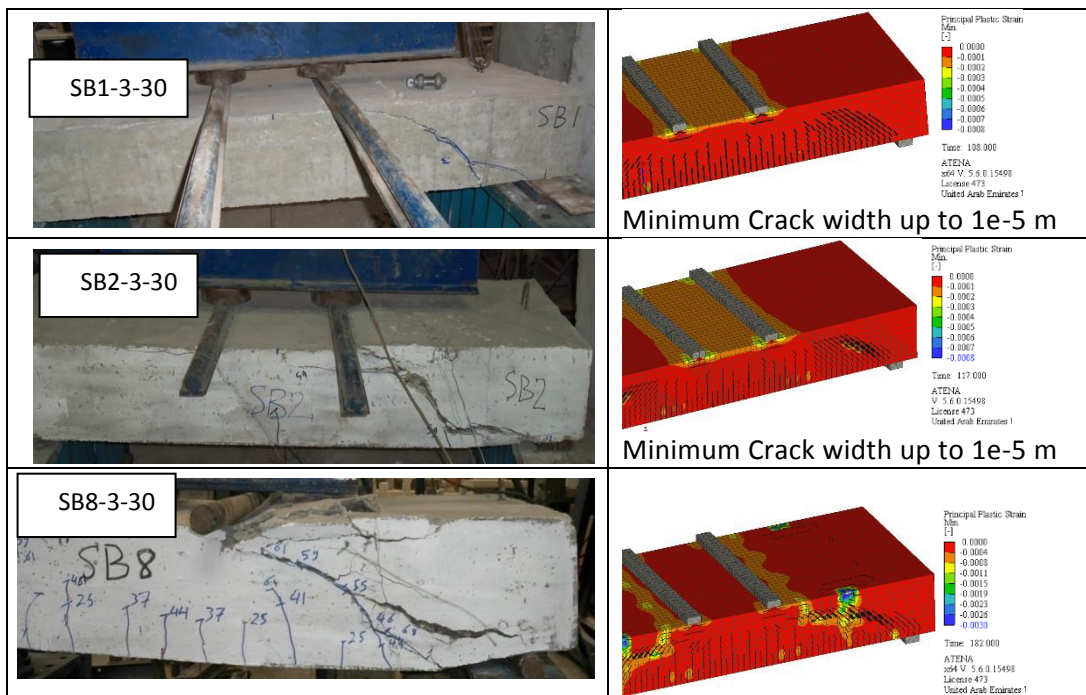


Fig. 3: Crack patterns of specimens of G1, experimental and numerical

3.3 Load- Deflection Relationship

Fig. 5 presents a comparison between the load-deflection curves predicted numerically and those obtained from the experimental tests for specimens of group G1. As it is seen, the agreement is reasonable. The validated FE models in the present study can serve as a good tool to simulate the nonlinear structural behavior of RC wide beams to investigate a wider range of parameters instead of laboratory testing, which is costly, time-consuming and labor-intensive.

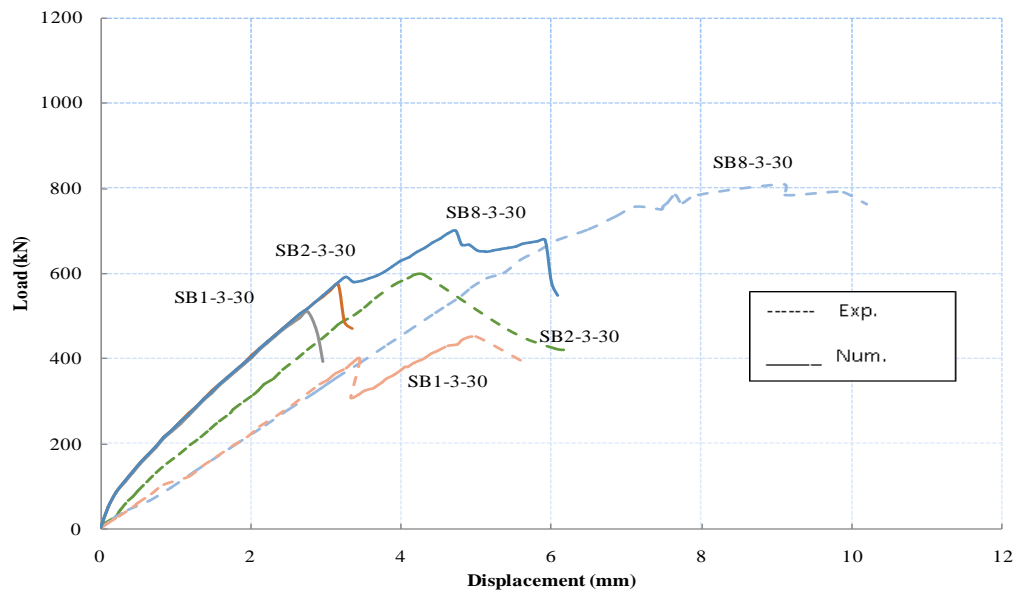


Fig. 5: Load- Deflection relationships of G1, experimental and numerical

3.4 Ductility

Ductility is the ability of the reinforced concrete member to sustain large inelastic deformations without excessive strength deterioration. The ductility can either be represented in terms of the ratio of maximum displacement to the yield displacement, both measured at mid span, or in terms of the displacement energy consumed by the specimen during the test measured as the area under the load displacement curve till the failure load which can be considered 80% of the ultimate load on the descending branch of the load-deflection curve. Since the flexure mode of failure was prevented for all specimens to allow for shear mode of failure, it was found more suitable to use the second measure of ductility. Table 1 shows the displacement energy values that are numerically measured for all specimens. It is undoubtedly noted that the increase in web reinforcement amount and yield stress generally increases the ductility and also, as the concrete strength increases, the ductility of specimens increases.

3.5 Strains in Web Reinforcement

Two electrical strain gages were attached to stirrups vertical branches of both SB2-3-30 and SB8-3-30. The experimental readings of the strain gauges in these specimens indicated that the transverse reinforcement developed yielding before failure of specimens and also entered the strain hardening range exhibiting strains much higher than the yield strain which indicates that the stirrups were successful in resisting the shear stresses in test specimens. Fig.6 plots the load- strain relationships of the vertical stirrups for SB8-3-30. Examining Fig.6, some of the strain gages output were compression with small values in the early loading stage and this may be attributed to applying the load on the top surface of the beams. However, strains of vertical stirrups of SB8-3-30 were also predicted numerically at the same points and compared with those measured experimentally in Fig. 6. The numerical and experimental tensile steel strain responses are in good agreement. The strains in SB2-3-30 were not recorded experimentally due to malfunction of the strain gauge prior to testing.

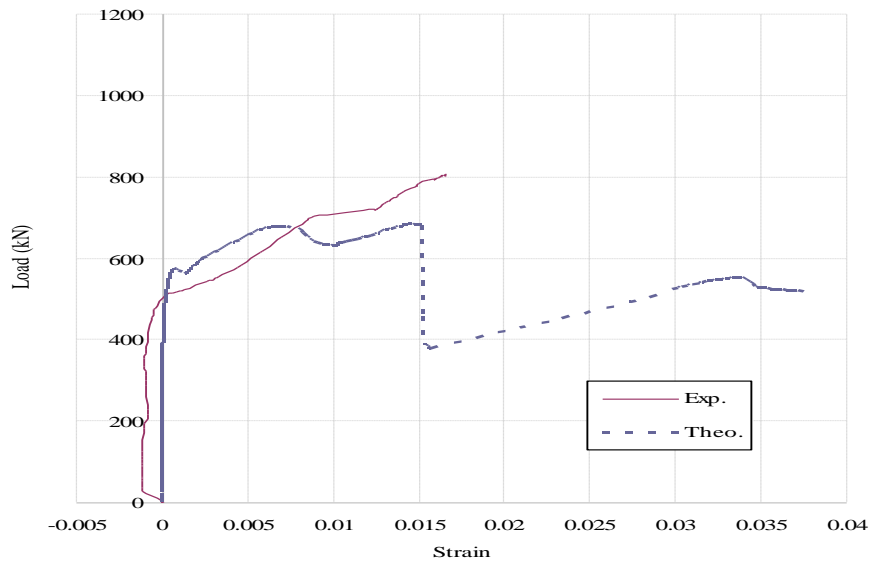


Fig.6. Comparison between numerically and experimentally recorded strain of steel stirrups for Beam SB8-3-30

4 EFFECTS OF KEY PARAMETERS

4.1 Effect of Web Reinforcement

The numerical load-deflection relationships of all groups are shown in Fig.7. The load-deflection curves of the specimens show that shear reinforcement had no significant impact on the deflection values at pre-cracking stage. On the other hand, the transverse reinforcement had noticeable impact on the ultimate load, the corresponding displacement and ductility. The enhancement increases with increasing the amount of stirrups. For example, the ultimate load of beams SB2-3-45 and SB8-3-45 is higher than SB1-3-45 by 6.2% and 31.5%, respectively. The ultimate load of beams SB2-3-60 and SB8-3-60 is higher than SB1-3-60 by 8.7% and 31%, respectively. Also, the ductility of SB2-3-45 and SB8-3-45 is higher than SB1-3-45 by 20.1% and 290%, respectively, indicating the fruitful effect of increasing the amount of stirrups, see Table 1. Beyond the ultimate load, the descending branch of the curves had a real relation with the existence and amount of web reinforcement. As shown in Fig. 7 and Table 1, high grade steel was more effective in the contribution of the shear strength and ductility of wide beams than mild type. In addition, it can be noticed that for a constant value of (a/d) , the gain or the relative enhancement in shear capacity due to web reinforcement was almost the same for different grades of concrete. It is obviously concluded that the effect of the transverse reinforcement in shear resistance of the wide beams should not be ignored.

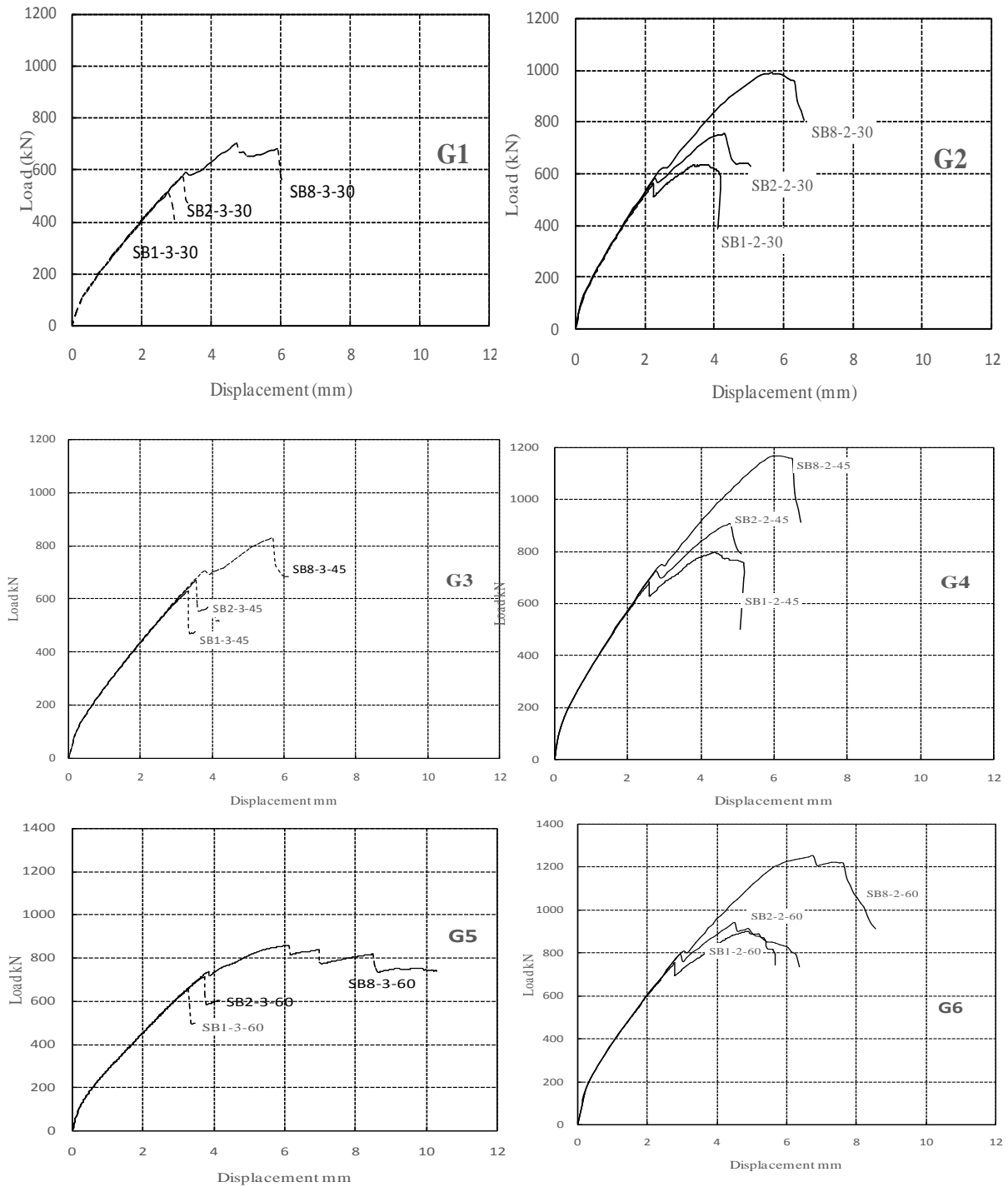


Fig. 7: Load- Deflection relationships of G1- G6, numerical prediction

4.2 Effect of Concrete Strength, f_{cu}

Predicted results of Groups G1 to G6 were analyzed to demonstrate the effect of concrete compressive strength on RC wide beams behavior. Concrete compressive strength was 30 MPa for Groups G1 and G2. It was 45 MPa for series G3 and G4 and it was 60 MPa for G5 and G6. Providing $(a/d) = 3.0$ and for specimens without web reinforcement, the ultimate shear resistance value increased by 23% and 29% by

increasing f_{cu} from 30 to 45 and 60, respectively, comparing with SB1-3-30. The increase was 18% and 22% when using R6/200 mm compared with SB2-3-30. In addition, the increase was 14% and 20% when using T10/200 mm compared with SB8-3-30 and this enhancement in shear strength is attributed to the increase in concrete compressive strength, Figs. 8-a, b, c. The same trend was noted for $(a/d) = 2$, Table 1.

On the other hand, it was observed that ductility increased in specimens with higher concrete grade as these specimens had higher ultimate load than specimens with lower concrete compressive strength. Providing $(a/d) = 3.0$ and for specimens without web reinforcement, the ductility increased by 42.9% and 50.6% by increasing f_{cu} from 30 to 45 and 60 MPa, respectively, comparing with SB1-3-30. The increase was 35.1% and 45.6% when using R6/200 mm compared with SB2-3-30. In addition, the increase was 27.8% and 40.2% when using T10/200 mm compared with SB8-3-30 and this enhancement in ductility is attributed to the increase in concrete compressive strength, Table 1.

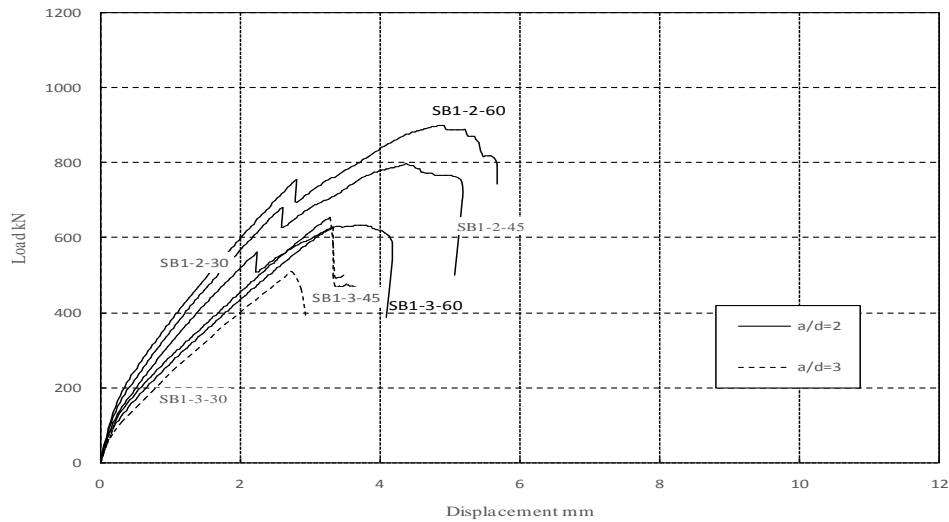


Fig. 8-a: Effect of concrete strength, no web reinforcement

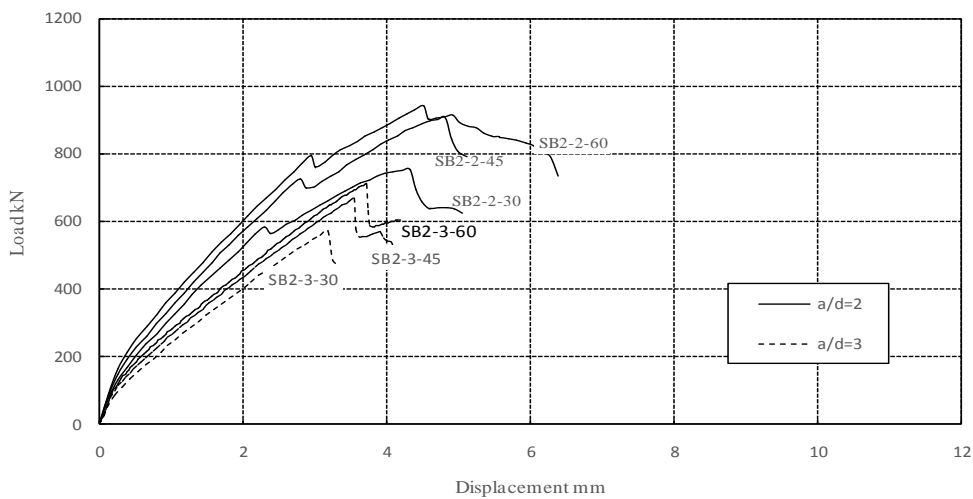


Fig. 8.b: Effect of concrete strength with R6/200 mm web reinforcement

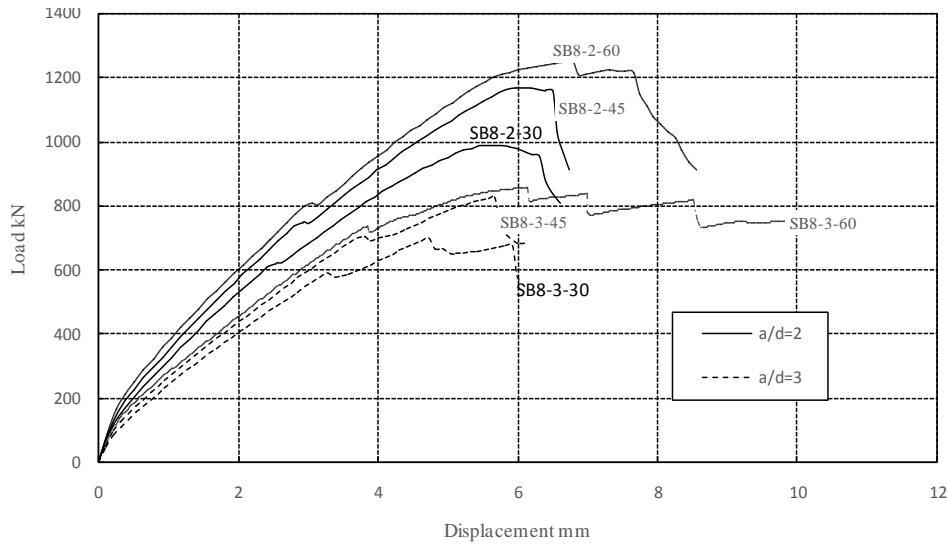


Fig. 8.c: Effect of concrete strength with T10/200 mm web reinforcement

4.3 Effect of Shear Span to Depth Ratio, (a/d)

Predicted results of Groups G1 to G6 were analyzed to demonstrate the effect of shear span to depth ratio (a/d) on RC wide beams behavior. The ratio was 3.0 for Groups G1, G3 and G5 and it was 2.0 for series G2, G4 and G6. Providing $f_{cu} = 30.0$ MPa and for specimens without web reinforcement, the ultimate shear resistance value increased by 24.8% by decreasing (a/d) from 3.0 to 2.0. The increase was 29% and 41% when using R6/200 mm and T10/200 mm, respectively, see Figs. 9-a, b, c and Table 1. Providing $f_{cu} = 45.0$ MPa and for specimens without web reinforcement, the ultimate shear resistance value increased by 26.9% by decreasing (a/d) from 3.0 to 2.0. The increase was 35.8% and 41% when using R6/200 mm and T10/200 mm, respectively. Providing $f_{cu} = 60.0$ MPa and for specimens without web reinforcement, the ultimate shear resistance value increased by 37.6% by decreasing (a/d) from 3.0 to 2.0. The increase was 32.3% and 46.1% when using R6/200 mm and T10/200 mm, respectively. This noticed enhancement in shear strength is attributed to the decrease in the ratio of (a/d).

However, the ductility increased by decreasing span-to-depth ratio (a/d) as shown in Figs. 9-a, b, c and Table 1. Providing $f_{cu} = 30$ MPa, the ductility value increased by 119%, 128 and 52% for web reinforcement of zero, R6/200 mm and T10/200 mm, respectively, by decreasing (a/d) from 2 to 3. Providing $f_{cu} = 45$ MPa, the ductility value increased by 141%, 109 and 41% for web reinforcement of zero, R6/200 mm and T10/200 mm, respectively, by decreasing (a/d) from 2 to 3. Providing $f_{cu} = 60$ MPa, the ductility value increased by 181%, 174 and 28% for web reinforcement of zero, R6/200 mm and T10/200 mm, respectively, by the same change of (a/d).

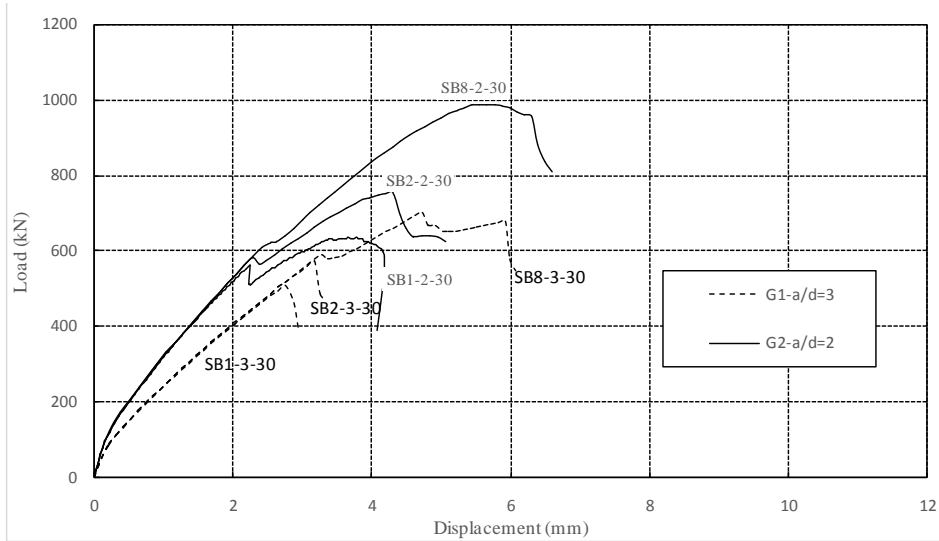


Fig. 9.a: Effect of (a/d), $f_{cu}=30$ MPa

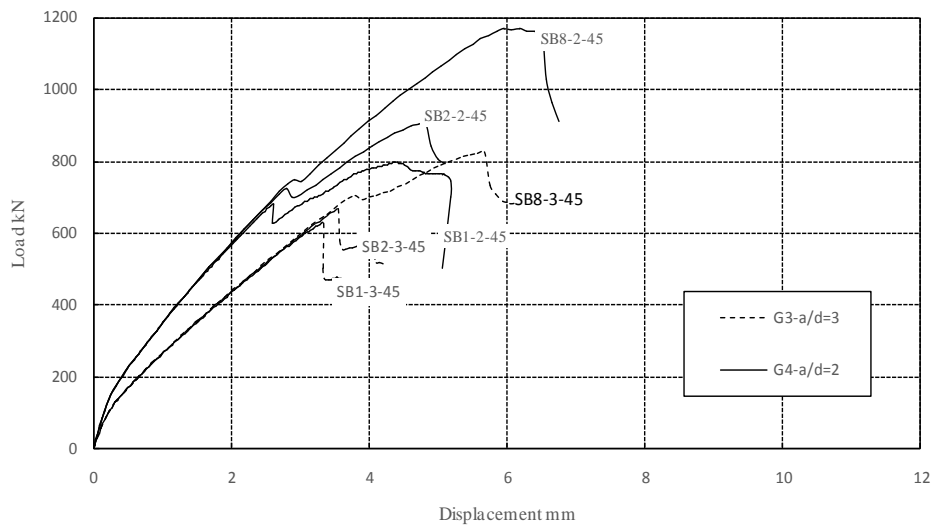


Fig. 9.b: Effect of (a/d), $f_{cu}=45$ MPa

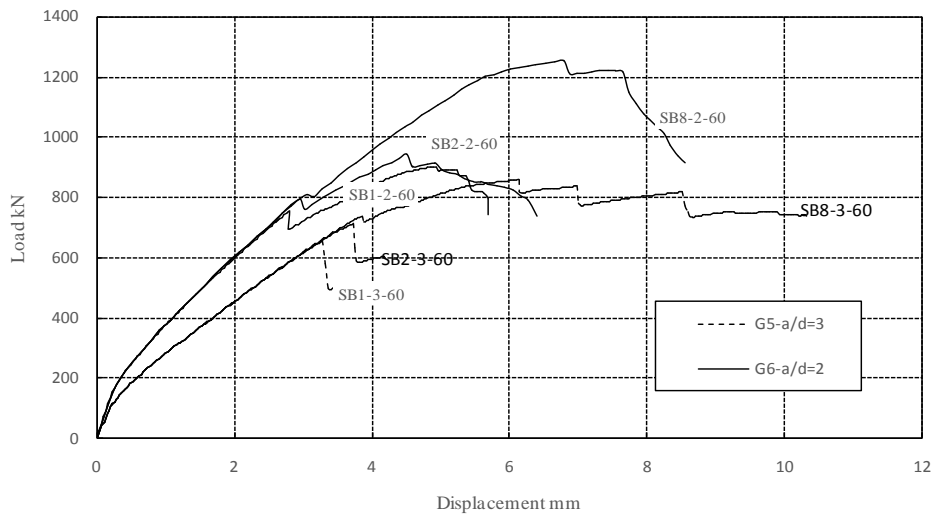


Fig. 9.c: Effect of (a/d), $f_{cu}=60$ MPa

5 CONCLUSIONS

Based on the study presented herein, the following conclusions have been drawn:

1. The accuracy and validity of the FE models developed in this study to predict the nonlinear response of RC wide beams was demonstrated by comparing their predictions with the experimental results in the literature. The nonlinear responses of the specimens predicted numerically were in very good agreement with those obtained from the experiments. The results may contribute to the future development of design guidelines for contribution of the shear reinforcement for wide beams in the Egyptian Concrete Code, ECP 203.
2. The FE models validated in the present study can serve as a powerful tool in future research to simulate the nonlinear structural behavior of RC wide beams and to investigate a wider range of parameters instead of laboratory testing, which is costly, time-consuming and labor-intensive.
3. Contribution of web reinforcement- in form of vertical stirrups- in shear strength and behavior of wide beams cannot be ignored. The effect of web reinforcement to the shear capacity is proportional to the amount of shear reinforcement.
4. The relative enhancement in shear capacity of RC wide beams due to web reinforcement was almost the same for different grades of concrete.
5. Increasing concrete compressive strength of RC wide beams increases the shear strength and ductility.
6. Increasing shear span-to-depth ratio (a/d) of RC wide beams decreases the shear strength and ductility.

Acknowledgment

The authors would like to thank Prof. Mohamed S. Issa for reviewing the paper before sending it for publication.

REFERENCES

- [1] A, S. Lubell; Evan, C. B. and Michael, P. C. Shear Reinforcement Spacing in Wide members. ACI Structural Journal. V.106, No.2, March-April 2009.
- [2] Sherwood, E. G.; Adam, S.L; Bentz, E. C.; and Collins, M. P. One-Way Shear Strength of Thick Slabs and Wide Beams. ACI Structural Journal, V. 103, No. 6, Nov.-Dec. 2006, pp. 794-802.
- [3] Dino, A.; Evan, C. B. and Michael, P. C. Effect of Concrete Strength and Minimum Stirrups on Shear Strength of Large Members. ACI Structural Journal, V. 98, No. 3, May-June 2001, pp. 291-300.
- [4] James, M. and James, K. W. Reinforced Concrete Exterior Wide Beam-Column-Slab Connections Subjected to Lateral Earthquake Loading. ACI Structural Journal. V.96. No.4, July-August1999. pp. 577- 585.

- [5] Building Code Requirements for Structural Concrete (ACI 318-08) and Commentary (318R-05),” American Concrete Institute, Farmington Hills, Mich.
- [6] Khalil, A.H.H. Shear Strength of Concrete Embedded Beams & Hollow Block Slabs. 4th international scientific conference of The Military Technical College, 2008.
- [7] S. E. Mohammadyan; A. K. Marsono; R. Abdullah and M. Moghadasi. Wide Beam Shear Behavior with Diverse Types of Reinforcement. ACI Structural Journal. V.111, No.6, Dec. 2014.
- [8] Egyptian Code of Practice for Design and Construction of Reinforced Concrete Structures, ECP203-2007. Housing and Building National Research Center, Giza, Egypt.
- [9] Said, M. and Elrakib. T. Enhancement of Shear Strength and Ductility for RC Wide Beams Due to Web Reinforcement. HBRC Journal, Vol. 9 , No.3, Dec. 2013
- [10] ATENA Program Documentation, Cervenka Consulting, Prague, Czech Republic, 2007.
- [11] CEB-FIP, CEB-FIP Model Code 1990. Bulletin of information, 213/214, Lausanne, Switzerland, 1993, pp. 33-51.
- [12] Van Mier J.G., Multiaxial strain-softening of concrete. Mater Struct. 19(3), 1986, pp 190–200.
- [13] European Committee for Standardization, Eurocode 2, Design of Concrete Structures– Part 1-1: General rules and rules for buildings, Brussels, Belgium, 2005, pp.94-103.
- [14] Vecchio, F.J., Collins, M.P. The modified compression-field theory for reinforced concrete elements subjected to shear. ACI J Proc, 83(2), 219-231, 1986.